PERGAMON

Aerosol Science 33 (2002) 17–34

Journal of
Aerosol Science

www.elsevier.com/locate/jaerosci

Titania formation by $TiCl_4$ gas phase oxidation, surface growth and coagulation

Patrick T. Spicer[a], Olivier Chaoul[b], Stavros Tsantilis[c], Sotiris E. Pratsinis[c,*]

[a] *The Procter and Gamble Company, Corporate Engineering Technologies, Beckett Ridge Technical Center, 8256 Union Centre Blvd., Cincinnati, OH 45069, USA*
[b] *Department of Chemical Engineering, University of Cincinnati, Cincinnati, OH 45221-0171, USA*
[c] *Department of Mechanical and Process Engineering, Institute for Process Engineering, Sonneggstrasse 3, ETH Zurich, CH-8092 Zurich, Switzerland*

Received 21 June 2000; accepted 4 May 2001

Abstract

Titania particle formation by $TiCl_4$ gas phase oxidation, surface growth and coagulation is investigated by a moving sectional population balance model. The dynamic evolution of the detailed particle size distribution is studied accounting for and neglecting the effect of surface growth. The effects of process temperature, T, and precursor volume fraction, ϕ, on the average diameter, d_p, and geometric standard deviation of the particle size distribution are highlighted. Accounting for surface reaction accelerates particle growth for $\phi > 0.01$ and gives a size distribution narrower than the self-preserving one as long as the precursor conversion is less than 99%. At higher conversions, the particle size distribution reaches the self-preserving limit corresponding to aerosols made by coagulation. A monodisperse model represents well aerosol dynamics at high process temperatures. A design diagram summarizing the significance of surface reaction in terms of ϕ and d_p at various process temperatures is presented.

1. Introduction

Titania is widely used as a pigment to increase the hiding power of paints, as a catalyst support (Tan, Dou, Lu, & Wu, 1991), and as a photocatalyst able to destroy organic pollutants (Ollis, Hsiao, Budiman, & Lee, 1984). The performance of titania in these applications is often a function of the particle size distribution (PSD). For example, the opacity of paints containing titania pigments depends on the average particle size and width of the PSD. In addition, the

* Corresponding author. Tel.: +41-1-632-3180; fax: +41-1-632-1595.
E-mail address: pratsinis@ivuk.mavt.ethz.ch (S. E. Pratsinis).

0021-8502/01/$ - see front matter
PII: S0021-8502(01)00069-6

Nomenclature

A	total particle area concentration (cm^2/cm^3)
C	$TiCl_4$ concentration (mol/cm^3)
$g(v)$	arbitrary function of particle volume v
$J(t)$	nucleation rate (# cm^3/s)
k_g	$TiCl_4$ gas phase reaction rate constant ($1/s$)
k_s	$TiCl_4$ surface reaction rate constant (cm/s)
k	$TiCl_4$ overall oxidation rate constant ($1/s$)
N_{av}	Avogadro's number ($1/mol$)
N	particle number concentration (# $1/cm^3$)
N_i	particle number concentration in the ith size bin (# $1/cm^3$)
$n(v,t)$	particle density for volume v and time t ($1/cm^6$)
$p(v)$	arbitrary function of particle volume v
P_i	integral value of $p(v,t)$ in the ith size bin
PSD	particle size distribution
$r_{critical}$	critical ratio of x_{i+1}/x_{i-1}
s	(initial) spacing factor (x_{i+1}/x_i)
T	temperature of the gas (K)
$u(v)$	arbitrary function of particle volume v defined as $p(v)g(v)$
v_g	average geometric volume defined by Eq. (20) (cm^3)
v_i	lower boundary point volume of bin i (cm^3)
v_m	$TiCl_4$ monomer volume (cm^3)
V	particle volume concentration (cm^3/cm^3)
x_i	representative grid point volume of bin i ($[v_{i+1} + v_i]/2$) (cm^3)

Greek letters

β	collision kernel for TiO_2 particles (cm^3/s)
ϕ	initial $TiCl_4$ volume fraction in a mixture of $TiCl_4$ and O_2 (dimensionless)
η_i	function defined by Eq. (9)
η	function defined by Eq. (11)
σ_{gn}	number-based geometric standard deviation of the PSD (dimensionless)
σ_{gv}	volume-based geometric standard deviation of the PSD (dimensionless)

activity of a catalyst is a function of the available surface area and thus the particle size distribution.

Typically, TiO_2 is made by the chloride process in aerosol reactors by the oxidation of $TiCl_4$. The oxidation reaction to titania can occur either in the gas phase and/or at the surface of existing titania particles. As a result, the relative rates of nucleation, coagulation, and surface reaction determine the evolution of the PSD and product titania powder. Warren and Seinfeld (1985) used a sectional (discretized) representation of the PSD to model the evolution of an aerosol during simultaneous nucleation, condensation, and coagulation. Although the

sectional technique provides an accurate description of aerosol coagulation (Gelbard, Tambour, & Seinfeld, 1980; Gelbard, & Seinfeld, 1980; Landgrebe, & Pratsinis, 1990), numerical dispersion occurs when accounting for condensation. Warren and Seinfeld (1985) showed that for growth by condensation of an initially monodisperse aerosol the sectional technique artificially broadened the PSD (which should have remained monodisperse) as particles entering a new section were distributed evenly within the new section (numerical diffusion). They also found that decreasing the sectional spacing could minimize numerical diffusion at the cost of significantly increased computational time.

The effects of numerical diffusion can be eliminated by the use of the moving sectional technique (Gelbard, 1990; Kim, & Seinfeld, 1990). In this technique, the previously fixed sections of the size distribution are allowed to move with time as growth occurs, thus preserving the exact characteristics of the PSD before condensation. Sher and Jokiniemi (1993) developed a moving sectional model describing simultaneous nucleation, coagulation and condensation in the containment of a nuclear reactor following an accidental release. Jacobson and Turco (1995) used a hybrid sectional model consisting of stationary sections to describe coagulation and moving sections to describe condensation and evaporation of a multiple component aerosol. While accurate, this algorithm requires specialized numerical techniques to solve the population balance efficiently. Kumar and Ramkrishna (1997) developed a moving sectional model describing simultaneous nucleation, coagulation and growth of particles. A varying number of sections is employed. While discretizations for coagulation and growth preserve the total number and volume of particles, their discretization for nucleation guarantees preservation of only the number as the mass may not always be conserved (Kumar & Ramkrishna, 1996a).

Xiong and Pratsinis (1991) modeled titania formation and growth by gas phase chemical reaction and coagulation, using sectional and lognormal moment models of the PSD for non-isothermal conditions. They showed that TiO_2 monomer inception by $TiCl_4$ chemical reaction is indistinguishable from nucleation. Jain, Kodas, Wu, and Preston (1997) concluded that surface reaction (Ghoshtagore, 1970; Ghoshtagore, & Noreika, 1970) does not affect the evolution of the titania particle size distribution when assuming that the titania size distribution is lognormal and that the $TiCl_4$ oxidation rate (Pratsinis, Bai, Biswas, Frenklach, & Mastrangelo, 1990) solely represents gas phase particle formation. Pratsinis and Spicer (1998) used a monodisperse model to examine the same system by assuming that the reaction rate constant of Pratsinis et al. (1990) encompasses both gas phase and surface reaction as the total $TiCl_4$ consumption rate was measured by FTIR. Using the surface reaction rate of Ghoshtagore (1970) they found that TiO_2 formation by surface and gas phase reaction always produced larger particles than by gas phase reaction alone. They also found good agreement between their model and literature data on the significance of surface reaction during TiO_2 formation.

A moving sectional discretization preserving particle volume and number for simultaneous nucleation, coagulation and surface growth is presented in this paper. The model by Kumar and Ramkrishna (1997), including a new discretization for nucleation, provides the basis for the present model simulating titania particle formation and growth by gas phase (Pratsinis et al., 1990; Pratsinis, & Spicer, 1998) and surface reaction (Ghoshtagore, 1970) of $TiCl_4$. Although a detailed moving sectional model was chosen here, a monodisperse model can also be attractive for the description of aerosol dynamics, primarily for its high computational speed (Warren, & Seinfeld, 1985; Landgrebe, & Pratsinis, 1990; Kruis, Kusters, Pratsinis, & Scarlett, 1993; Panda,

& Pratsinis, 1995). Monodisperse models are frequently used when interfacing fluid with particle dynamics of industrial processes (Schild, Gutsch, Muhlenweg, & Pratsinis, 1999; Johannessen, Pratsinis, & Livbjerg, 2000) or large scale air pollution. The predictions of a monodisperse model are also evaluated here as the sectional model can be quite demanding in computation time.

2. Theory

2.1. Reaction model

The formation of TiO_2 takes place by the overall reaction of $TiCl_4$ with O_2:

$$TiCl_4 + O_2 \rightarrow TiO_2 + 2Cl_2.$$

The depletion of $TiCl_4$ occurs by both homogeneous gas phase reaction and by the reaction at the surface of existing TiO_2 particles:

$$\frac{dC}{dt} = -kC = -(k_g + k_s A)C, \tag{1}$$

where C (mol/cm^3) is the concentration of $TiCl_4$, t (s) is the residence time, A (cm^2/cm^3) is the surface area concentration of TiO_2 particles, k (1/s) is the overall oxidation rate constant of $TiCl_4$ (Pratsinis et al., 1990):

$$k = 8.26 \times 10^4 \exp\left(\frac{-10,681}{T}\right), \tag{2}$$

while k_g (1/s) is the gas phase reaction rate constant, T (K) is the process temperature and k_s (cm/s) is the surface reaction rate constant (Ghoshtagore, 1970; Pratsinis, & Spicer, 1998):

$$k_s = 4.9 \times 10^3 \exp\left(\frac{-8,993}{T}\right). \tag{3}$$

2.2. Monodisperse model

Assuming that the size distribution of the aerosol remains monodisperse throughout the process, the evolution of the total aerosol number, N (particles/cm^3) and volume, V (cm^3/cm^3) concentration is given by (Pratsinis, & Spicer, 1998):

$$\frac{dN}{dt} = k_g C N_{av} - \frac{\beta N^2}{2} = (k - k_s A) C N_{av} - \frac{\beta N^2}{2}, \tag{4}$$

$$\frac{dV}{dt} = kCN_{av} v_m, \tag{5}$$

where N_{av} is Avogadro's number, v_m (cm^3) is the volume of a TiO_2 monomer ($\sim 3.32 \times 10^{-23}$ cm^3), and β (cm^3/s) is the monodisperse collision frequency for coagulation spanning over the free-molecular, transition and continuum regimes (Fuchs, 1964). Furthermore, β is a function of the average particle diameter given as d_p (cm) $= [(6/\pi)\,(V/N)]^{1/3}$ (Pratsinis, &

Spicer, 1998). The first right hand side (RHS) term in Eq. (4) represents the formation of particles by gas phase oxidation while the second RHS term represents the depletion of particle number concentration by coagulation. In Eq. (5), the RHS term represents the formation of aerosol volume by gas phase and surface oxidation of $TiCl_4$. When surface reaction is neglected, Eq. (4) becomes

$$\frac{dN}{dt} = kCN_{av} - \frac{\beta N^2}{2}, \tag{6}$$

whereas, Eq. (5) remains unchanged so that the same particle mass is produced. Finally, it should be noted that both monodisperse and sectional predictions are based on particle diameters of average volume, for the comparison to be consistent.

2.3. Moving sectional population balance model

The change in the number of particles in the size section i, N_i, by nucleation and coagulation is simulated using

$$\frac{dN_i}{dt} = \left.\frac{dN_i}{dt}\right|_{nuc} + \left.\frac{dN_i}{dt}\right|_{coag}, \tag{7}$$

where the subscripts denote the phenomenon causing a change in particle number concentration. It should be noted that surface growth has no effect on N_i. More specifically, the contributions from nucleation and coagulation are given as (Kumar, & Ramkrishna, 1997, 1996a):

$$\left.\frac{dN_i}{dt}\right|_{nuc} = J(t)\eta_i = (k_g CN_{av})\eta_i, \tag{8}$$

where

$$\eta_i = \begin{cases} 1, & v_m \in [v_i, v_{i+1}], \\ 0, & v_m \notin [v_i, v_{i+1}] \end{cases} \tag{9}$$

and

$$\left.\frac{dN_i}{dt}\right|_{coag} = \sum_{x_{i-1} \leqslant x_j + x_k \leqslant x_{i+1}}^{i \geqslant j \geqslant k} \left(1 - \frac{1}{2}\delta_{j,k}\right) \eta \beta_{j,k} N_j N_k - N_i \sum_{k=1}^{M} \beta_{i,k} N_k, \tag{10}$$

where

$$\eta = \begin{cases} \dfrac{x_{i+1} - (x_j + x_k)}{x_{i+1} - x_i}, & x_i \leqslant x_j + x_k \leqslant x_{i+1}, \\ \dfrac{x_{i-1} - (x_j + x_k)}{x_{i-1} - x_i}, & x_{i-1} \leqslant x_j + x_k \leqslant x_i. \end{cases} \tag{11}$$

In the above equations, M is the total number of sections (bins), ranging from 50 to 75 with an initial spacing factor s of 1.7, x_i (cm^3) is the pivot volume in section i with boundaries v_i and v_{i+1} and $\beta_{j,k}$ (cm^3/s) is the collision frequency function between particles in pivots j and k,

spanning over the free-molecular, transition, and continuum regimes (Fuchs, 1964; Phillips, 1975; Seinfeld, 1986). In addition, $\beta_{j,k}$ is a function of the characteristic diameters $d_{p,j}$, $d_{p,k}$, which for the present case of full coalescence upon collision, represent diameters of average volume $d_{p,j} = [(6/\pi)x_j]^{1/3}$. Eq. (11) is a simplification of the general equation shown in Kumar and Ramkrishna (1997), representing here the case of preservation of mass and numbers. For the case of surface growth, pivots x_i change with time based on the governing surface reaction law (Kumar, & Ramkrishna, 1997):

$$\left.\frac{\mathrm{d}V_i}{\mathrm{d}t}\right|_{\mathrm{surf}} = N_i \left.\frac{\mathrm{d}x_i}{\mathrm{d}t}\right|_{\mathrm{surf}} = k_{\mathrm{s}} C A_i N_{\mathrm{av}} v_{\mathrm{m}} \Rightarrow \left.\frac{\mathrm{d}x_i}{\mathrm{d}t}\right|_{\mathrm{surf}} = \frac{k_{\mathrm{s}} C A_i N_{\mathrm{av}} v_{\mathrm{m}}}{N_i} = \frac{k_{\mathrm{s}} C (N_i \pi d_{p,i}^2) N_{\mathrm{av}} v_{\mathrm{m}}}{N_i}. \tag{12}$$

For an arbitrary grid of x_i pivots (Kumar, & Ramkrishna, 1996a) Eqs. (7) and (12), describe aerosol dynamics for nucleation, coagulation and surface growth and are solved using the DIVPAG subroutine in IMSL (1980). However, when nucleation and surface growth occur simultaneously, the smallest bin containing the TiO_2 monomers will grow by surface reaction, leaving no bin with the same volume as a monomer to receive any subsequently formed nuclei. This results in a loss of accuracy in the numerical solution for the smallest particle sizes. To remedy this, a new bin is created, at sufficiently small time steps Δt, with its grid point equal to the monomer volume (Kumar, & Ramkrishna, 1997). The resolution of the PSD is examined over the particle size domain and unnecessary grid points are collapsed.

Although the above technique, introduced by Kumar and Ramkrishna (1997), correctly accounts for the number of monomers (nuclei), it does not always represent the total mass of incoming nuclei correctly, as no equation for the effect of nucleation on the pivot of the first section is included. In general (as the pivot $x_{i=1}$ moves away from v_{m} by surface growth), the total monomer mass can be considerably overpredicted unless very short time steps are taken, in the expense of computation time. Therefore, a different approach is followed here for the effect of nucleation on the evolution of pivots, $\mathrm{d}x_i/\mathrm{d}t$, that preserves both mass and numbers (Chaoul, 2000). More specifically, the general dynamic equation for pure nucleation is written as

$$\left.\frac{\partial n(v,t)}{\partial t}\right|_{\mathrm{nuc}} = J(t)\delta(v - v_{\mathrm{m}}). \tag{13}$$

Based on the moving pivot technique of Kumar and Ramkrishna (1996b; Section 2) two properties of the PSD, $p(v)$ and $u(v)$ [$\equiv g(v)p(v)$], are now desired to be preserved; $p(v)$ and $u(v)$ are arbitrary volume functions usually defined as moments of the PSD. When multiplying by $p(v)$ or $u(v)$ Eq. (13), and integrating between v_i and v_{i+1}, the rates of change of $p(v)n(v,t)$ and $u(v)n(v,t)$ in the ith bin are, respectively:

$$\left.\frac{\mathrm{d}P_i}{\mathrm{d}t}\right|_{\mathrm{nuc}} = \frac{\mathrm{d}}{\mathrm{d}t}\int_{v_i}^{v_{i+1}} p(v)n(v,t)\,\mathrm{d}v = p(v_{\mathrm{m}})J(t)\eta_i, \tag{14}$$

$$\left.\frac{\mathrm{d}U_i}{\mathrm{d}t}\right|_{\mathrm{nuc}} = \frac{\mathrm{d}}{\mathrm{d}t}\int_{v_i}^{v_{i+1}} u(v)n(v,t)\,\mathrm{d}v = u(v_{\mathrm{m}})J(t)\eta_i. \tag{15}$$

From the definition of pivot x_i (Kumar, & Ramkrishna, 1996b) $U_i = g(x_i)P_i$ and thus $\mathrm{d}U_i/\mathrm{d}t = g(x_i)\mathrm{d}P_i/\mathrm{d}t + P_i\,\mathrm{d}g(x_i)/\mathrm{d}t$. Combining this with Eqs. (14) and (15) gives

$$\left.\frac{\mathrm{d}g(x_i)}{\mathrm{d}t}\right|_{\mathrm{nuc}} = \frac{1}{P_i}[u(v_{\mathrm{m}}) - g(x_i)\,p(v_{\mathrm{m}})]J(t)\eta_i. \tag{16}$$

For the preservation of the total number and volume of particles, $p(v) = 1$, $u(v) = g(v) = v$. Under these conditions Eq. (14) correctly reproduces Eq. (8) while Eq. (16) simplifies to

$$\left.\frac{\mathrm{d}x_i}{\mathrm{d}t}\right|_{\mathrm{nuc}} = \frac{1}{N_i}(v_{\mathrm{m}} - x_i)J(t)\eta_i = \frac{1}{N_i}(v_{\mathrm{m}} - x_i)(k_{\mathrm{g}}CN_{\mathrm{av}})\eta_i. \tag{17}$$

Consequently, the total change of x_i is now given by

$$\frac{\mathrm{d}x_i}{\mathrm{d}t} = \left.\frac{\mathrm{d}x_i}{\mathrm{d}t}\right|_{\mathrm{nuc}} + \left.\frac{\mathrm{d}x_i}{\mathrm{d}t}\right|_{\mathrm{surf}}. \tag{18}$$

The system of differential equations to be solved now includes Eqs. (7) and (18) while the grid regeneration principles remain virtually the same as in Kumar and Ramkrishna (1997). In general, the goal is to regenerate the grid without decreasing the accuracy of the calculations and to maintain a rather geometric resolution, as this guarantees low computational demands for a wide range of particle sizes; thus for instance, pivot x_i is eliminated when the ratio of the adjacent pivots x_{i+1}/x_{i-1} is smaller than a critical value $r_{\mathrm{critical}} = s^{1.5}$. The difference of the present model (Eqs. (7) and (18)) with respect to that of Kumar and Ramkrishna (1997) stems from the introduction of Eq. (17) in which N_i acts as an inertia term (the bigger the N_i is, the less the average volume x_i changes). In conclusion, Eq. (17) systematically adjusts pivot volume by accounting for the changes created by the incoming monomers, thus allowing for the preservation of both mass and numbers without necessarily decreasing the time step, Δt.

For the case of pure gas phase chemical reaction, the surface reaction rate, k_{s}, is set to zero. At high precursor concentrations, the rate of $TiCl_4$ consumption by surface reaction may exceed the rate predicted by Eq. (2). In this case, the overall rate of reaction is taken as $k_{\mathrm{s}}A = k_{\mathrm{s}}\sum_i A_i = k_{\mathrm{s}}\sum_i(\pi d_{p,i}^2)N_i$ (only surface oxidation occurs) and $k_{\mathrm{g}} = 0$ so that the mass balance is preserved.

In the following sections, predictions of the sectional model will be discussed in terms of average diameter

$$\left(\frac{6\sum_i N_i x_i}{\pi\sum_i N_i}\right)^{1/3} \tag{19}$$

and volume-based geometric standard deviation (Landgrebe, & Pratsinis, 1990: Eqs. B[4] and B[7] by replacing $n(v,t)$, N_k and N with $vn(v,t)$, $V_k \equiv N_k x_k$ and V, respectively) using the appropriate definition of the density function, $n(v,t) = \sum_i N_i\delta(v - x_i)$ (Kumar, & Ramkrishna, 1997):

$$\ln^2\sigma_{\mathrm{gv}} = \frac{1}{9}\int_0^{+\infty}\frac{vn(v,t)}{V}\ln^2\left(\frac{v}{v_{\mathrm{g}}}\right)\mathrm{d}v = \frac{1}{9}\sum_i\frac{x_i N_i}{V}\ln^2\left(\frac{x_i}{v_{\mathrm{g}}}\right),$$

$$V = \int_0^{+\infty} vn(v,t)\,\mathrm{d}v = \sum_i x_i N_i \quad \text{and} \quad \ln v_{\mathrm{g}} = \int_0^{+\infty}\frac{vn(v,t)}{V}\ln v\,\mathrm{d}v = \sum_i\frac{x_i N_i}{V}\ln x_i. \tag{20}$$

3. Results and discussion

3.1. Model validation and selection of simulation conditions

The most important characteristic of a moving sectional model (Eqs. (7) and (18)) is its elimination of numerical diffusion (Gelbard, 1990). The prediction of the moving sectional model (Eqs. (7) and (18)) was evaluated for the evolution of an initially monodisperse size distribution by condensation only at a constant growth rate. The distribution remained perfectly monodisperse independent of time as the moving sections closely followed the growth of the particles. For the coagulation of spherical particles, the model predicted the correct asymptotic (self-preserving) geometric standard deviations of the number size distribution in the free-molecular ($\sigma_{gn} = 1.463$) and the continuum regimes ($\sigma_{gn} = 1.446$) in agreement with Vemury and Pratsinis (1995). When coagulation occurs at a constant rate ($\beta_0 = 7.7 \times 10^{-10}$ cm^3/s) and condensation is a function of particle volume ($7.7 \times 10^4 v_i$), an analytical solution (Gelbard, & Seinfeld, 1978) can be compared with the predictions of the numerical model. These predictions were in agreement with that analytical solution, indicating that the model is robust and accurate. A validation of the sectional model (Eqs. (7) and (18)) was also carried out for the case of simultaneous nucleation and growth (Chaoul, 2000), by adapting a similar test case from Hounslow, Ryall, and Marshall (1988).

3.2. Evolution of TiO_2 particle size distribution

Synthesis of TiO_2 by gas phase or surface oxidation of $TiCl_4$ is investigated at atmospheric pressure, $T = 1000$–1800 K and $\phi = 0.0001$–0.5 in oxygen carrier gas (Pratsinis, & Spicer, 1998). Fig. 1a shows the evolution of the titania particle size distribution (PSD) with time at $T = 1400$ K and $\phi = 0.1$ neglecting surface reaction ($k_s = 0$). Initially, a large number ($\sim 10^{14}$/cm^3) of TiO_2 monomers (molecules with radius ~ 0.40 nm) is homogeneously formed by gas phase oxidation of $TiCl_4$. These monomers then grow by coagulation into larger particles, broadening the PSD so that only after 0.001 s a bimodal distribution exists composed of fine and coarse particles. At long times (over 1 s), the PSD reaches its self-preserving form.

When surface oxidation is considered for $\phi = 0.1$ (Fig. 1b), the evolution of the particle size distribution is initially similar to that observed in Fig. 1a, as a monodisperse PSD is formed by gas phase oxidation, followed by growth by coagulation into larger size classes. At these conditions, the initial bimodal distribution exists for a very short time. As the available particle surface area reaches a certain level and the reaction (nucleation) mode disappears ($t \leqslant 0.01$ s) in contrast to Fig. 1a, surface oxidation dominates over gas phase oxidation (primary nucleation). At this point the PSD is dominated by surface growth and becomes even narrower than that of the self-preserving distribution ($t = 0.1$ s). However, at later times ($t = 1$ s) the self-preserving distribution is attained.

Fig. 2 shows the evolution of (a) the average particle diameter (of average volume) and (b) the volume-based geometric standard deviation σ_{gv} neglecting (broken line) and accounting for (continuous line) surface reaction. In the latter case a sharp increase of the average diameter (caused by surface growth) can be observed between $t = 10^{-3}$ and 10^{-2} s. Between 0.004 and 0.1 s, the PSD has become unimodal as was shown in Fig. 1b. Then, the surface area of the

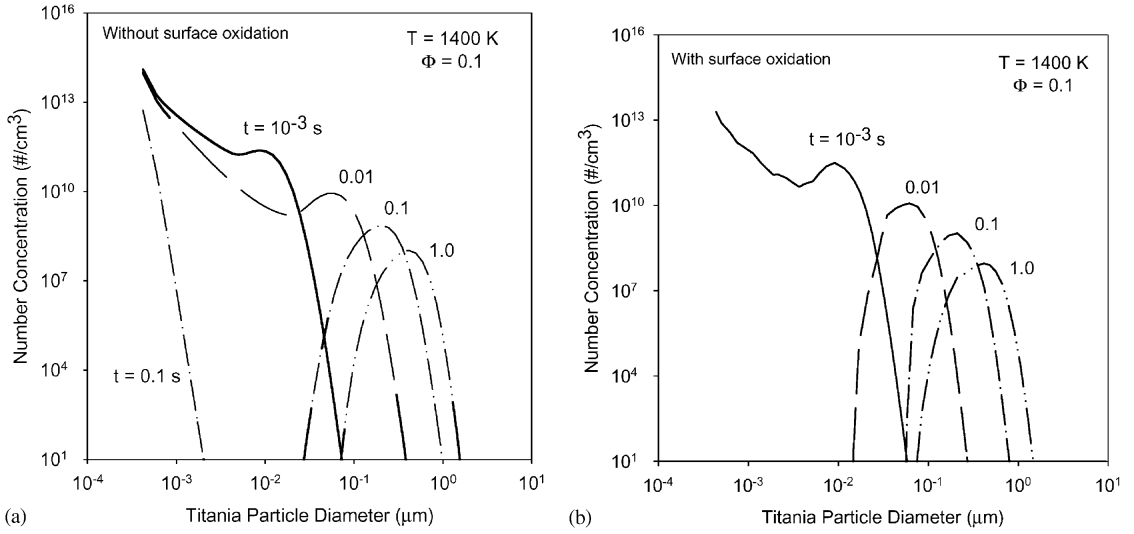

Fig. 1. Time evolution of the titania particle size distribution (PSD) by $TiCl_4$ gas phase oxidation at $T = 1400$ K and $\phi = 0.1$ (a) neglecting and (b) accounting for surface oxidation. The distribution broadens by coagulation from initially monodisperse conditions. Accounting for surface reaction accelerates particle growth.

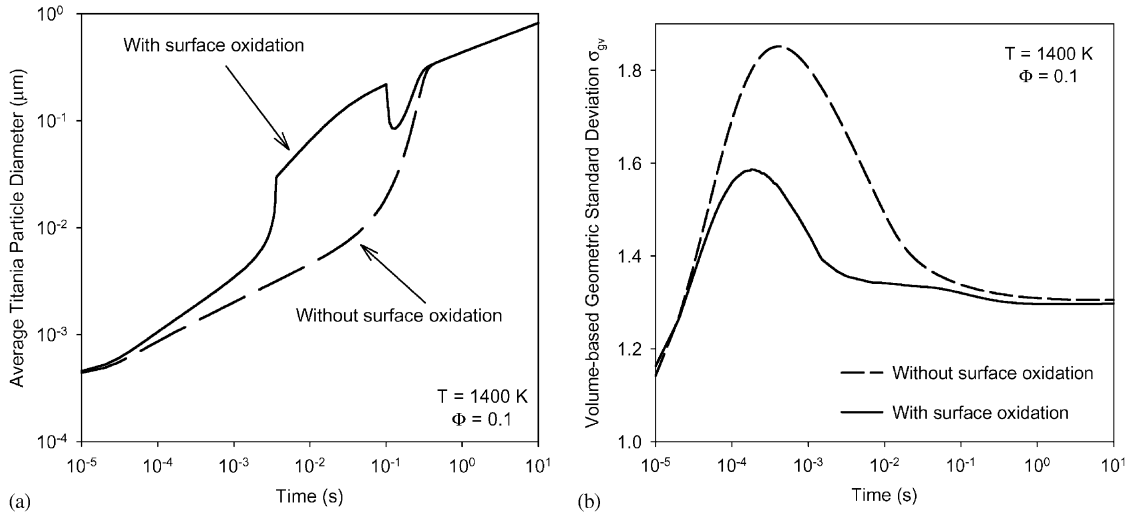

Fig. 2. Evolution of the (a) average titania particle diameter, (b) volume-based geometric standard deviation of the titania PSD for $T = 1400$ K and $\phi = 0.1$. Accounting for surface oxidation produces larger titania particles and narrower product particle size distribution especially at $TiCl_4$ conversion less than 99% (here $t < 0.1$ s).

particles decreases by coagulation but increases by surface growth. The low concentration of the remaining $TiCl_4$ at $t = 0.1$ s results in a slow increase of the total particulate surface area by surface reaction which is unable to compensate for the area loss by coagulation. Thus, a new reaction (secondary nucleation) by gas phase oxidation takes place. This burst causes a

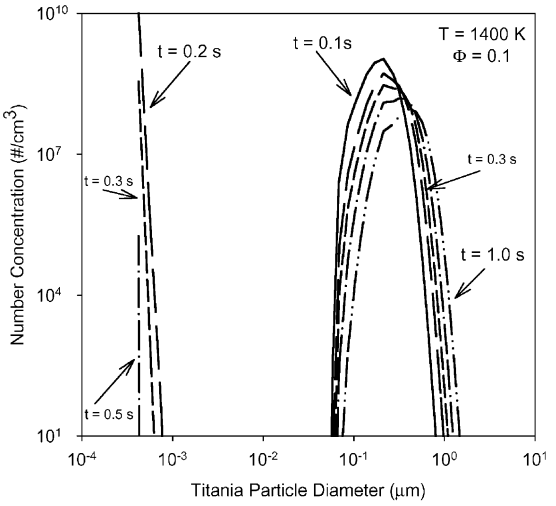

Fig. 3. Time evolution of the titania PSD by gas phase and surface oxidation for $T = 1400$ K and $\phi = 0.1$ during a reaction (nucleation) burst. A transient reaction (nucleation) mode is observed to appear and disappear between 0.1 and 1 s.

rapid decrease of the average particle diameter at about $t = 0.1$ s followed by an increase at 0.3 s (Fig. 2a).

Fig. 2b shows the evolution of the volume-based geometric standard deviation. Neglecting or accounting for surface reaction results in the same qualitative features for σ_{gv} in both cases: A peak between $t = 10^{-4}$ and 10^{-3} s corresponds to the onset of the coagulation mode and its equivalence with the nucleation mode with respect to TiO_2 mass at these early times. Second, both cases converge to the self-preserving limit as dictated by coagulation at long times. Under all conditions accounting for surface growth leads to narrower PSDs. However, the advantage of surface growth for narrowing the PSD is achieved at residence times that correspond to precursor ($TiCl_4$) conversions less than 99%.

Fig. 3 shows the detailed evolution of the PSD for $t = 0.1$–1.0 s. After the secondary nucleation burst ($t = 0.1$–0.2 s) the number of particles in the reaction (nucleation) mode greatly exceeds those in the coagulation mode. Due to the $TiCl_4$ depletion, the nucleation mode rapidly decreases (Fig. 3) after the nucleation burst, and an increase of the average titania particle diameter (Fig. 2a) takes place while the volume based σ_{gv} is not affected by this secondary nucleation. For $t > 0.5$ s, the reaction (nucleation) mode has disappeared by coagulation (scavenging) of particles in the coagulation mode (0.05–2 μm).

3.3. Effect of $TiCl_4$ mole fraction, ϕ, on particle diameter and polydispersity

Fig. 4a shows the evolution of the average particle diameter from $t = 10^{-5}$–10 s for initial mole fractions of $\phi = 0.01$ and 0.5 at 1400 K accounting for the surface reaction (solid lines)

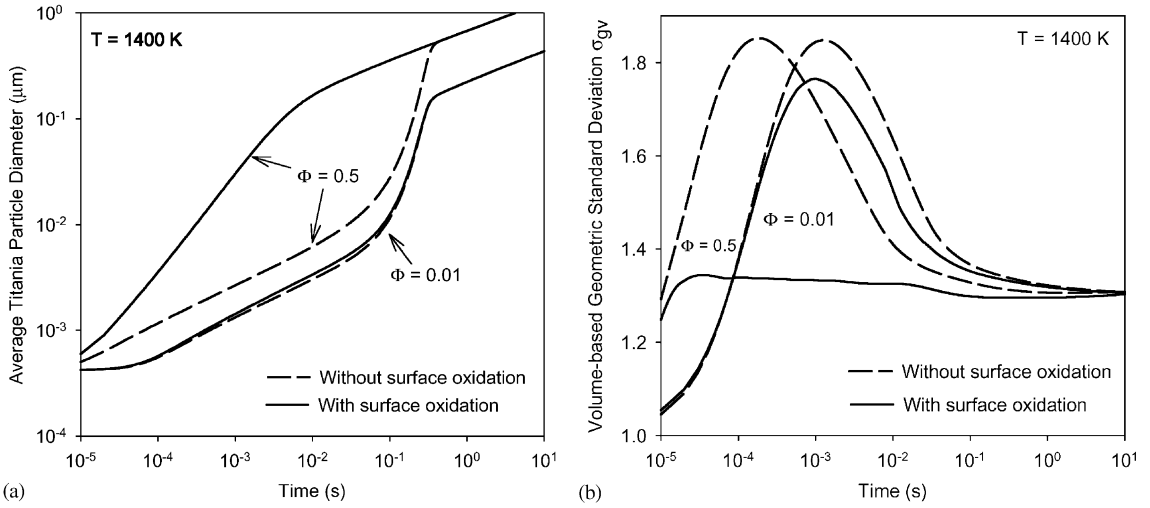

Fig. 4. Effect of $TiCl_4$ (mole fraction) concentration, ϕ, on the evolution of (a) the average particle diameter and (b) the volume-based geometric standard deviation, σ_{gv} of the titania PSD for $T = 1400$ K and $\phi = 0.01$ and 0.5. Increasing the $TiCl_4$ concentration increases the rate of particle formation, providing sufficient surface area for dominance of surface oxidation.

and neglecting it (broken lines). At low $TiCl_4$ concentrations (ϕ close to 0.01), accounting for surface reaction affects little the particle size distribution. Gas phase reaction and coagulation clearly dominate particle formation and growth at this and lower $TiCl_4$ mole fractions at all times. A small region of difference between the two cases is observed for $\phi = 0.01$ between $t = 10^{-4}$ and 0.1 s that results from the competition between surface and gas phase oxidation (Fig. 4a). At early times and low ϕ, surface oxidation begins to increase the average particle diameter above that for pure gas phase oxidation but is negligible as new particles continue to form.

At higher $TiCl_4$ concentrations ($\phi = 0.5$) which are typical for industrial conditions, the significance of surface reaction is increased because of the abundance of available surface area of freshly formed TiO_2 for surface oxidation of $TiCl_4$. As a result, at $t = 0.1$ s and $\phi = 0.5$, the average titania particle diameter accounting for surface reaction is 350 nm while neglecting it gives a d_p of only 27 nm.The high surface area of the particles during the process prevents the onset of reaction (nucleation) bursts and modes. Our simulations have shown that the late nucleation burst takes place for ϕ less than 0.15–0.2.

Fig. 4b shows the evolution of the volume-based geometric standard deviation for the same conditions as in Fig. 4a. For $\phi = 0.01$, little difference exists between both cases. Increasing the $TiCl_4$ fraction to $\phi = 0.5$ significantly increases the importance of surface oxidation. At these conditions, when accounting for surface reaction (solid line) the volume-based geometric standard deviation remains nearly constant and smaller than that predicted when surface reaction is neglected. It is worth noting that for $t < 0.1$ s corresponding to $d_p < 10$ nm (Fig. 4a, $\phi = 0.5$, broken line) the PSD is significantly narrower when accounting for surface reaction than when neglecting it. Of course, at long durations the self-preserving limit is reached again.

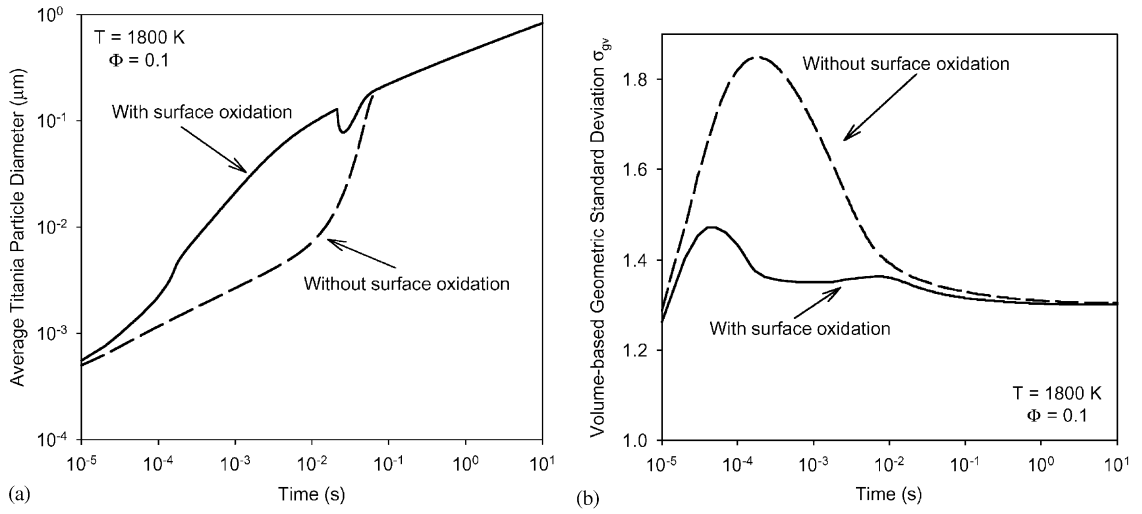

Fig. 5. Effect of process temperature on the evolution of (a) the average particle diameter, (b) volume-based geometric standard deviation of the titania PSD for $T = 1800$ K and $\phi = 0.1$. Increasing the temperature increases the surface and gas phase oxidation kinetics, significantly accelerating particle growth by surface reaction.

It should be noted that the assumption of complete particle coalescence leads to underprediction of the aerosol area since anisotropic aggregates have larger area than equivalent spheres. However, accounting for the greater surface area of aggregates will only enhance the trends already shown here with respect to the dominance of particle surface reaction over gas phase oxidation. This is currently investigated in our laboratories.

Fig. 5 shows the evolution of the (a) average particle diameter and (b) volume-based geometric standard deviation of the PSD for initial $TiCl_4$ mole fraction $\phi = 0.1$ and $T = 1800$ K. Increasing the process temperature accelerates the $TiCl_4$ gas phase and surface oxidation kinetics as well as the coagulation rate of TiO_2 particles. As a result, a more rapid increase of the average particle size is observed in Fig. 5a as the process temperature is set to 1800 K. However, it should be noted that for long residence times the asymptotic particle diameter in the self-preserving limit depends very little on the process temperature. The time-lag needed to attain self-preserving conditions in terms of σ_{gn} (corresponding to the convergence of the simulations accounting for and neglecting surface reaction) is reduced by an order of magnitude for $T = 1800$ K (Fig. 5b) compared to 1400 K and for $T = 1400$ K compared to 1000 K.

3.4. Comparison with monodisperse model results

Although the moving sectional model provides a robust description of TiO_2 formation and growth, the average computational load required (e.g. 12 h for the simulation shown in Fig. 1b, in a 200 MHz Pentium PC) makes it worth examining the predictions of a monodisperse model of TiO_2 aerosol synthesis (the corresponding computation time in this case is just a few minutes). Fig. 6a shows the predictions of the monodisperse and population balance models for $T = 1800$ K and $\phi = 0.1$. The monodisperse model underpredicts the particle

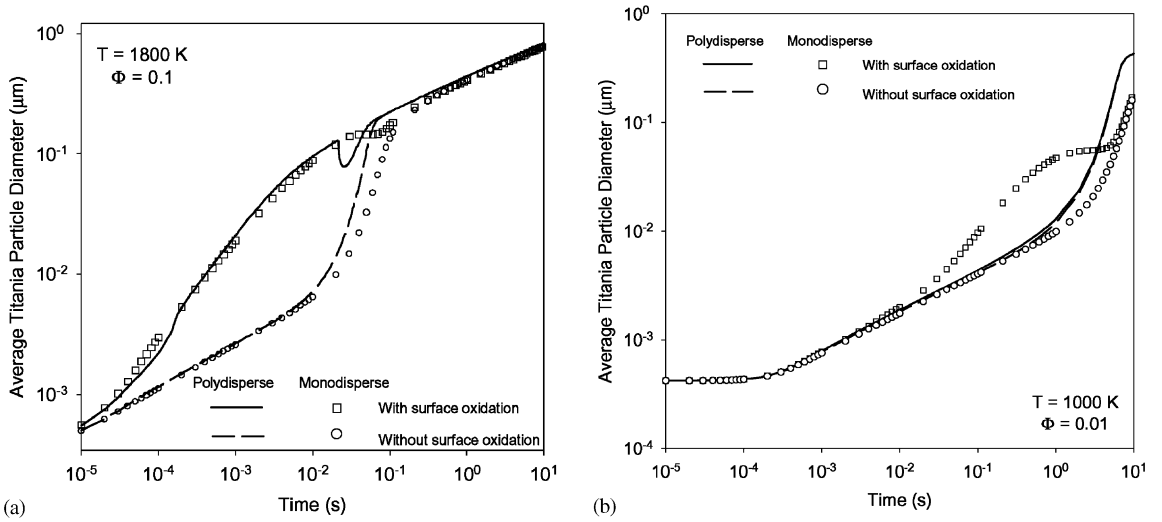

Fig. 6. Evolution of the average titania particle diameter accounting or neglecting for surface oxidation of $TiCl_4$ using the polydisperse and monodisperse models for (a) $T = 1800$ K, $\phi = 0.1$ and (b) $T = 1000$ K and $\phi = 0.01$. The models are in good agreement ($T = 1800$ K) when a unimodal distribution has been formed but differ at low reactant conversions when both reaction and coagulation modes are significant.

diameter when neglecting surface oxidation as coagulation of polydisperse aerosols is faster than that of monodisperse ones (Hinds, 1982). However, when surface oxidation is considered, the monodisperse model slightly overpredicts the particle diameter, predicting even a broader range of time when surface oxidation is dominant. A monodisperse model overpredicts the significance of surface reaction because it underpredicts initial particle growth by coagulation, leading to an enhanced surface area and consequently an overprediction of the surface reaction rates (Warren, & Seinfeld, 1985). As a result, no late nucleation burst is detected with the monodisperse simulation.

Fig. 6b shows a comparison of the monodisperse and polydisperse models at $T = 1000$ K and $\phi = 0.01$. While the polydisperse simulation shows a negligible effect of surface oxidation reaction mechanisms, the monodisperse model shows a difference of an order of magnitude at $t = 1$ s in the predicted average particle diameters when surface oxidation is neglected and accounted for. For the latter case, the underprediction of coagulation rates in the monodisperse model leads to erroneous overpredictions of the total surface area of the particles and thus of the surface oxidation rates. For long residence times, the average particle diameter is underpredicted in the monodisperse model as coagulation is the only dominant process. This indicates the limitations of monodisperse models.

Fig. 7 shows a synthetic comparison of the monodisperse and polydisperse model predictions with surface oxidation at $T = 1000, 1400$ and 1800 K. For $T = 1400$ and 1800 K, the average particle diameters predicted by the two models at $t = 10$ s agree within 10% relative difference. At $T = 1000$ K, this difference is at least 40% for all the considered cases. This discrepancy at low temperatures and good agreement for higher temperatures are caused by the reaction kinetics and their effect on coagulation. At 1400 and 1800 K, the nucleation mode created by chemical

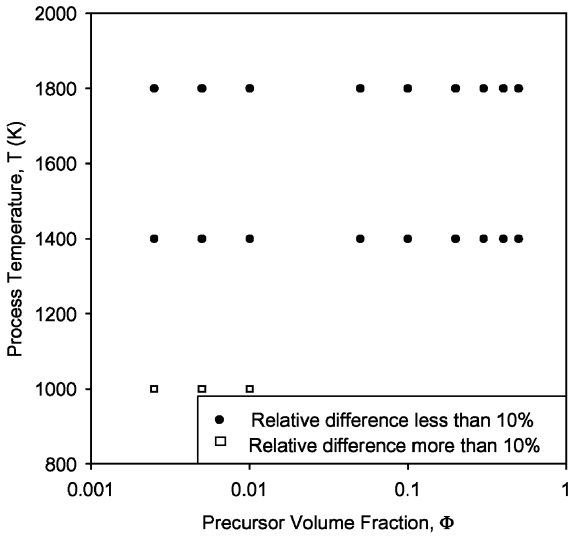

Fig. 7. Synthetic comparison of the monodisperse and polydisperse models with respect to their prediction of the particle diameter in the process parameter space of T and ϕ and long residence times ($t = 10$ s). Monodisperse models compare well with polydisperse at high $TiCl_4$ conversion ($>99\%$).

reaction of the precursor disappears after 1 s. As a result, a relatively narrow unimodal PSD is observed in the polydisperse simulations. The dynamics of such a PSD are well approximated by a monodisperse model, although the coagulation kinetics are underpredicted. At $T = 1000$ K, the creation of monomers by chemical reaction persists well after $t = 1$ s. In the polydisperse model, these monomers are scavenged by bigger particles and the PSD is bimodal. In the monodisperse model, the creation of monomers only lowers the average particle diameter. Clearly, at slow reaction rates that give rise to bimodal size distributions, the monodisperse model does not approximate well the PSD dynamics because it underestimates the coagulation rate. Another consequence of this approximation is an overprediction of the surface oxidation kinetics as seen in Fig. 6b. In conclusion, monodisperse models are accurate when a unimodal PSD is quickly reached (Landgrebe, & Pratsinis, 1990).

Fig. 8 evaluates the significance of the overall $TiCl_4$ oxidation rate form used here (solid line), and of that given by Jain et al. (1997) (dash and dot line). Fig. 8 shows that the latter assumption underpredicts the significance of surface oxidation. This result, along with the use of a lognormal approximation of the PSD, may explain the conclusion of Jain et al. (1997) that surface oxidation was insignificant in TiO_2 production by $TiCl_4$ oxidation at all conditions. While the lognormal model of Jain et al. (1997) allows for the consideration of particle polydispersity, its assumption of a lognormal PSD limits its ability to describe particle behavior following a nucleation burst. As monomers form by gas phase reaction, then grow by coagulation, a bimodal PSD is formed (Figs. 1 and 3) that is not well described by moment techniques as has been shown by Xiong and Pratsinis (1991). Finally, it should be noted that when surface growth is neglected, both cases give the same results (broken line) as now only one (gas phase) reaction occurs (Pratsinis et al., 1990).

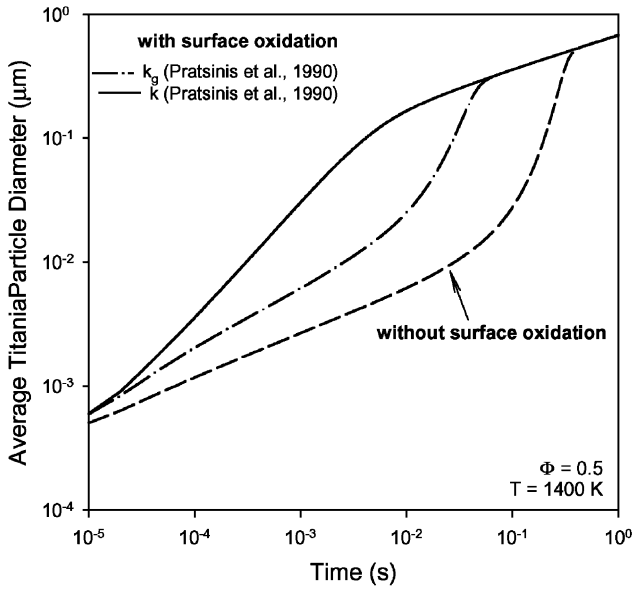

Fig. 8. Comparison of alternative descriptions of the chemical reaction on the evolution of titania particle diameter by $TiCl_4$ oxidation accounting for and neglecting surface reaction at $T = 1400$ K and $\phi = 0.5$. Line (–·–), k_g (Pratsinis et al., 1990), k_s (Ghoshtagore, 1970), and $k = k_g + k_s A$; line (——), k_s (Ghoshtagore, 1970), k (Pratsinis et al., 1990) and $k_g = k - k_s A$; line (– – –), $k_s = 0$, $k = k_g$ (Pratsinis et al., 1990).

3.5. Diagram for dominance of gas phase and surface oxidation of $TiCl_4$

Fig. 9 shows the contour lines for which a minimum of 5% difference is found in the particle diameters calculated neglecting and accounting for surface reaction. The contour lines are shown for $T = 1400$ and 1800 K as these are used for titania synthesis. The characteristic U shape of the contour lines can be explained using Fig. 2a. The left hand side of the curves corresponds to early divergence between the process simulations when the particulate area is sufficient to significantly reduce the gas phase oxidation rate. As ϕ increases, more particles and thus more area is created during the early stages of reaction and the particle diameters in Fig. 9 tend towards the monomer diameter. The right hand side of the curves corresponds to late convergence as predicted by the self-preserving theory, when coagulation becomes the only remaining particulate process and the precursor is depleted. When ϕ decreases, surface reaction becomes less significant. As a result, the time needed for the two simulations to diverge increases and the convergence time decreases. At very low ϕ ($\sim 10^{-3}$), the effect of accounting for surface reaction is almost negligible. Thus, the convergence and divergence times tend towards equal values and lower volume fractions cannot be defined as the difference in predicted particle diameters becomes less than 5% during the entire residence time. Increasing the temperature decreases both chemical reaction time and the time lag needed to attain self-preserving conditions. Consequently, the curves show a shift to lower particle diameters.

In addition to the boundaries from the present model, Fig. 9 shows the contour line for $T = 1400$ K using the monodisperse model of Pratsinis and Spicer (1998). Although the

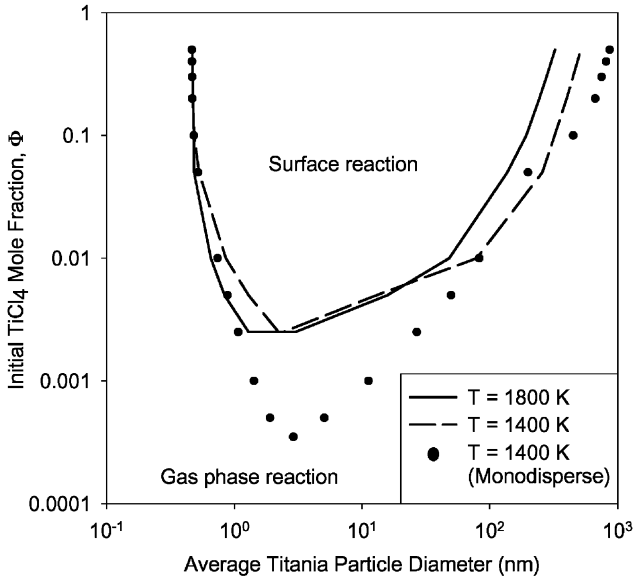

Fig. 9. Regions of $TiCl_4$ mole fraction and product TiO_2 diameter in which surface growth or gas phase reaction and coagulation dominate at 1400 and 1800 K with the present polydisperse model (lines) and the monodisperse model (symbols) at 1400 K. Above the contours narrower particle size distributions are produced for $TiCl_4$ conversion $<99\%$ as a result of the dominance of surface reaction over gas phase oxidation.

predicted curve retains the characteristic U shape observed with the polydisperse model, it shows a minimum lower by an order of magnitude. This difference can be explained by the different coagulation rate predicted by monodisperse and polydisperse simulations. In monodisperse models surface oxidation kinetics are artificially enhanced and a smaller ϕ (than in polydisperse calculations) is necessary to create a divergence between simulations neglecting and accounting for surface oxidation.

4. Conclusions

The competition between gas phase and surface $TiCl_4$ oxidation reaction for the synthesis of TiO_2 was investigated using a moving sectional population balance model that eliminated numerical diffusion errors while accounting for simultaneous nucleation, coagulation, and surface reaction. Accounting for surface reaction in models of TiO_2 formation increases the average particle size for inlet $TiCl_4$ volume fraction $\phi > 0.01$ compared to neglecting surface reaction. Narrower product titania PSDs are obtained when accounting for surface reaction as long as the $TiCl_4$ conversion is less than 99%. This effect is amplified with increasing process temperature. The population balance model is shown to be in good agreement with a monodisperse model of TiO_2 formation and growth in most cases, although the monodisperse model overpredicts the effect of surface oxidation at low T and ϕ. A diagram for the significance of surface growth in terms of process T, product particle diameter and inlet $TiCl_4$ volume fraction was developed.

Acknowledgements

Support by the US National Science Foundation, Grant # CTS-9619392, the Ohio Board of Regents and the Swiss National Science Foundation, Grant # 2100-055469.98/1, is gratefully acknowledged.

References

Chaoul, O. (2000). *Aerosol process simulation by fixed and moving sectional techniques*. Department of Chemical Engineering, University of Cincinnati, Cincinnati, OH 45221-0171, USA.

Fuchs, N. A. (1964). *The mechanics of aerosols*. Elmsford, NY: Pergamon Press.

Gelbard, F., & Seinfeld, J. H. (1978). Numerical solution of the dynamic equation for particulate systems. *Journal of Computational Physics*, *28*, 357.

Gelbard, F., & Seinfeld, J. H. (1980). Simulation of multicomponent aerosol dynamics. *Journal of Colloid and Interface Science*, *78*, 485.

Gelbard, F. (1990). Modeling multicomponent aerosol particle growth by vapor condensation. *Aerosol Science and Technology*, *12*, 399.

Gelbard, F., Tambour, Y., & Seinfeld, J. H. (1980). Sectional representations for simulating aerosol dynamics. *Journal of Colloid and Interface Science*, *76*, 541.

Ghoshtagore, R. N. (1970). Mechanism of heterogeneous deposition of thin film rutile. *Journal of Electrochemical Society: Solid State Science*, *117*, 529.

Ghoshtagore, R. N., & Noreika, A. J. (1970). Growth characteristics of rutile film by chemical vapor deposition. *Journal of Electrochemical Society: Solid State Science*, *117*, 1310.

Hinds, W. C. (1982). *Aerosol technology*. New York: Wiley-Interscience.

Hounslow, M. J., Ryall, R. L., & Marshall, V. R. (1988). A discretized population balance for nucleation, growth and aggregation. *A.I.Ch.E. Journal*, *34*, 1821.

IMSL, . (1980). *IMSL contents document*, (8th ed.) Houston: International Mathematical and Statistical Libraries.

Jacobson, M. Z., & Turco, R. P. (1995). Simulating condensation growth, evaporation, and coagulation of aerosols using a combined moving and stationary size grid. *Aerosol Science and Technology*, *22*, 73.

Jain, S., Kodas, T. T., Wu, M. K., & Preston, P. (1997). Role of surface reaction in aerosol synthesis of titanium dioxide. *Journal of Aerosol Science*, *28*, 133.

Johannessen, T., Pratsinis, S. E., & Livbjerg, H. (2000). Computational fluid-particle dynamics for the flame synthesis of alumina particles. *Chemical Engineering Science*, *55*, 177.

Kim, Y. P., & Seinfeld, J. H. (1990). Simulation of multicomponent aerosol condensation by the moving sectional method. *Journal of Colloid and Interface Science*, *135*, 185.

Kumar, S., & Ramkrishna, D. (1996a). On the solution of population balance equations by discretization—I. A fixed pivot technique. *Chemical Engineering Science*, *51*, 1311.

Kumar, S., & Ramkrishna, D. (1996b). On the solution of population balance equations by discretization—II. A moving pivot technique. *Chemical Engineering Science*, *51*, 1333.

Kumar, S., & Ramkrishna, D. (1997). On the solution of population balance equations by discretization—III. Nucleation, growth and aggregation of particles. *Chemical Engineering Science*, *52*, 4659.

Kruis, F. E., Kusters, K., Pratsinis, S. E., & Scarlett, B. (1993). A simple model for the evolution of the characteristics of aggregate particles undergoing coagulation and sintering. *Aerosol Science and Technology*, *19*, 514.

Landgrebe, J. D., & Pratsinis, S. E. (1990). A discrete-sectional model for powder production by gas-phase chemical reaction and aerosol coagulation in the free-molecular regime. *Journal of Colloid and Interface Science*, *139*, 63.

Ollis, D. F., Hsiao, C. -Y., Budiman, L., & Lee, C. -L. (1984). Heterogeneous photoassisted catalysis: Conversions of perchloroethylene, dichloroethane, chloroacteic acids, and chlorobenzenes. *Journal of Catalysis*, *88*, 89.

Panda, S., & Pratsinis, S. E. (1995). Modeling the synthesis of aluminum particles by evaporation-condensation in an aerosol flow reactor. *Nanostructured Materials*, *5*, 755.

Phillips, W. F. (1975). Drag on a small sphere moving through a gas. *Physics Fluids*, *18*, 1089.

Pratsinis, S. E., Bai, H., Biswas, P., Frenklach, M., & Mastrangelo, S. V. R. (1990). Kinetics of $TiCl_4$ Oxidation. *Journal of American Ceramics Society*, *73*, 2158.

Pratsinis, S. E., & Spicer, P. T. (1998). Competition between gas phase and surface oxidation of $TiCl_4$ during synthesis of TiO_2 particles. *Chemical Engineering Science*, *53*, 1861.

Schild, A., Gutsch, A., Mühlenweg, H., & Pratsinis, S. E. (1999). Simulation of nanoparticle production in premixed aerosol flow reactors by interfacing fluid mechanichs and particle dynamics. *Journal of Nanoparticle Research*, *1*, 305.

Seinfeld, J. H. (1986). *Atmospheric chemistry and physics of air pollution*. New York: Wiley.

Sher, R., & Jokiniemi, J. (1993). NAUAHYGROS 1.0: A code for calculating the behaviour of aerosols in nuclear plant containments following a severe accident. User's manual: EPRI TR-102775.

Tan, Y. -S., Dou, L. -Q., Lu, D. -S., & Wu, D. (1991). Coated silica as support for platinum catalyst I. Coating of silica with alumina, titania, and lanthana. *Journal of Catalysis*, *129*, 447.

Vemury, S., & Pratsinis, S. E. (1995). Self-preserving size distributions of agglomerates. *Journal of Aerosol Science*, *26*, 175 and erratum in *26*, 701.

Warren, D. R., & Seinfeld, J. H. (1985). Prediction of aerosol concentration resulting from a burst of nucleation. *Journal of Colloid and Interface Science*, *105*, 136.

Xiong, Y., & Pratsinis, S. E. (1991). Gas phase production of particles in reactive turbulent flows. *Journal of Aerosol Science*, *22*, 637.